RSC Advances

PAPER

View Article Online
View Journal | View Issue

Cite this: *RSC Adv.*, 2021, **11**, 22756

Received 4th February 2021
Accepted 18th June 2021

DOI: 10.1039/d1ra00942g

rsc.li/rsc-advances

Synthesis of a metal–organic framework by plasma in liquid to increase reduced metal ions and enhance water stability†

Moriyuki Kanno,* Takashi Kitao, Tsuyohito Ito* and Kazuo Terashima

Synthesis of a metal–organic framework by plasma in liquid was demonstrated with HKUST-1 as an example. HKUST-1 synthesized by this method contains a higher amount of monovalent copper ions than that synthesized by other conventional methods. The enhanced water stability was also confirmed.

Metal–organic frameworks (MOFs) are a class of hybrid materials composed of organic linkers and metal nodes. They have high surface areas with tunable pore size and functionality.[1,2] Because of these features, MOFs have potential applications in the fields of gas adsorption/storage,[3,4] catalysis,[5,6] drug delivery,[7,8] and fabrication of luminescent materials.[9,10] Many methods have been proposed for synthesizing MOFs; these include solvothermal methods,[11,12] microwave-assisted methods,[13,14] ultrasonic-assisted methods,[15,16] mechanochemical methods,[17] and electrosynthesis methods.[18] Different synthesis methods result in the different crystallinity and size. Further, the synthesis method can influence the physicochemical and semiconductor properties.[19]

Recently, a method for synthesizing MOFs in liquid contacting gas-phase dielectric barrier discharges has been reported.[20,21] However, MOFs synthesized by plasma have not been sufficiently characterized yet, thereby demanding further research. Plasma is a unique reaction field and has the advantage of being able to reduce and functionalize species using electrons and radicals. These characteristics have been widely utilized even in liquid phase for the synthesis of various materials such as carbon materials[22,23] and metal nanoparticles[24,25] and for introducing functional groups in materials.[26] Using plasma, it may be possible to synthesize functional MOFs with reduced metal ions or additional functional groups. Plasma in liquid generally have higher density of electrons and radicals than plasma in the gas phase,[27] and the influence of reactive species can be observed more prominently.

In this study, we focused on $[Cu_3(BTC)_2]_n$ (BTC = 1,3,5-benzenetricarboxylate). This is known as HKUST-1 and is one of the most widely researched MOFs. This MOF is assembled from copper nodes and BTC, with each copper coordinated with four oxygen atoms. HKUST-1 is a promising candidate for applications such as H_2 and SO_2 storage.[28,29] However, the crystal structure of HKUST-1 is changed by water molecules, and its surface area decreases.[30,31] To ensure the practical applications of HKUST-1, it is important to increase its resistance to water. To improve its stability to water, strategies such as incorporation of other materials, including graphite oxide[32] and carboxyl-functionalized attapulgite,[33] have been developed. In the post-processing using plasma, the adsorption of water molecules on HKUST-1 is inhibited by introducing hydrophobic groups with perfluorohexane.[34] In another method, the adsorption of water molecules on unsaturated metal sites was prevented by irradiating the HKUST-1 with oxygen plasma.[35] In addition, to improve the water tolerance, reduction of Cu(II) ions in HKUST-1 was also proposed.[36] However, in the above-mentioned methods, mixing of other materials or post-treatment steps was essential.

In this work, we synthesized HKUST-1 containing Cu(I) by plasma in liquid; the method involved *in situ* plasma treatment during the synthesis activated also by plasma. Its resistance to water was compared with HKUST-1 synthesized by conventional methods such as heating or addition of triethylamine at room temperature.

HKUST-1 was synthesized using the plasma generated by applying a bipolar pulse voltage to the electrode in an ethanol–water solution containing copper nitrate trihydrate and BTC (Fig. S1 and S2†). Hereafter in this paper, the thus-synthesized HKUST-1 will be referred to as PL-HKUST-1. For comparison, HKUST-1 was synthesized by the conventional heating method and by the addition of triethylamine at room temperature,[19] and the HKUST-1 formed are referred to as CH-HKUST-1 and RT-HKUST-1, respectively. The details of the synthetic methods are described in the ESI.†

All the samples were characterized by X-ray diffraction (XRD) and thermogravimetric analysis. The XRD patterns of CH-HKUST-1, RT-HKUST-1, and PL-HKUST-1 are shown in Fig. 1.

Department of Advanced Materials Science, Graduate School of Frontier Sciences, The University of Tokyo, 5-1-5 Kashiwanoha, Kashiwa, Chiba, 277-8561, Japan. E-mail: moriyuki.kanno@plasma.k.u-tokyo.ac.jp; tsuyohito@k.u-tokyo.ac.jp

† Electronic supplementary information (ESI) available: Synthesis methods of PL-HKUST-1, CH-HKUST-1 and RT-HKUST-1, instruments for characterization, and supplementary figures. See DOI: 10.1039/d1ra00942g

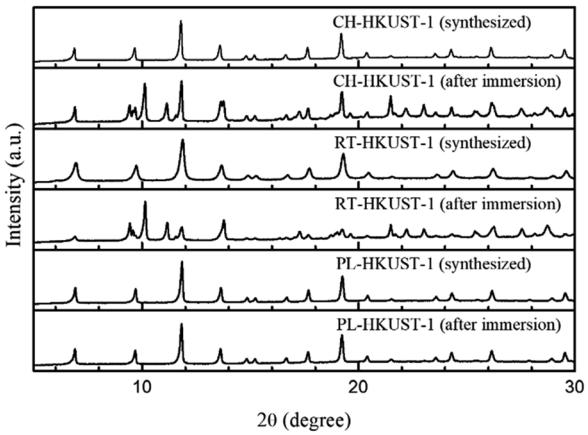

Fig. 1 XRD patterns of CH-HKUST-1, RT-HKUST-1, and PL-HKUST-1 before and after immersion in water.

In all the cases, the characteristic diffraction peaks of HKUST-1 were identified, confirming the phase-pure formation of HKUST-1 samples irrespective of the synthetic method.[37,38] Thermogravimetric analysis of HKUST-1 revealed that the thermal stability of PL-HKUST-1 was similar to those of CH-HKUST-1 and RT-HKUST-1 (Fig. S3†).

Fig. 2 shows the fluorescence (FL) spectra of CH-HKUST-1, RT-HKUST-1, and PL-HKUST-1 upon excitation at 310 nm at room temperature. Note that a broad peak around 520 nm was observed only for PL-HKUST-1 and not for CH-HKUST-1 and RT-HKUST-1. Such a behavior has been previously reported for Cu(I) complexes and is attributed to the metal-to-ligand charge transfer (MLCT) from Cu(I) to an empty antibonding π* orbital of the ligand.[39–42] Thus, the FL spectrum indicates that a certain amount of Cu(I) is formed in PL-HKUST-1, which highly contrasted to CH-HKUST-1 and RT-HKUST-1.

The existence of Cu(I) in PL-HKUST-1 was also confirmed by X-ray photoelectron spectroscopy (XPS). The XPS spectrum of PL-HKUST-1 showed peaks at 932.2 and 934.6 eV, assignable to Cu(I) and Cu(II), respectively (Fig. S4†).[43,44] Although the reduction to Cu(I) inevitably proceeded upon X-ray irradiation,[45] the concentration of Cu(I) in PL-HKUST-1 was apparently higher than those in CH-HKUST-1 and RT-HKUST-1, which was consistent with the FL spectra. The plasma has ample free electrons and ions, which can reduce metal ions *via* electrochemical reactions.[46] The temperature of the plasma in liquid could be as high as 1000–7000 K,[27] and the reduction of Cu(II) to Cu(I) by heat might occur.[47]

To examine the water stability of the MOFs, HKUST-1 was immersed in water at room temperature for 12 h. The XRD patterns of the samples after immersion in water were compared with those of the as-synthesized samples. The water treatment resulted in the appearance of new peaks at $2\theta \approx 9.4°$–$9.7°$, $10.1°$, $11.1°$, $17.3°$, and $19.6°$ for CH-HKUST-1 and RT-HKUST-1 (Fig. 1). Notably, the XRD patterns of PL-HKUST-1 before and after immersion in water were identical, with no detectable changes.

The effect of water treatment on the morphology of HKUST-1 was also investigated using scanning electron microscopy (SEM). Particles with octahedral shape were obtained by the plasma in liquid method, similar to those obtained by the conventional heating method (Fig. 3). After immersion in water, the formation of particles with a thread-like morphology was observed for CH-HKUST-1 and RT-HKUST-1, suggesting the decomposition of HKUST-1.[30,48] In contrast, although PL-HKUST-1 contained a portion of the etched corners, the particle shape and size remained unchanged after water treatment.

Fourier transform infrared (FTIR) spectra of HKUST-1 before and after the water treatment are shown in Fig. 4. All as-synthesized samples showed the typical characteristic peaks of HKUST-1. The bands from 1300 to 1700 cm^{-1} are associated with the carboxylate group of the BTC ligand.[49] The two peaks in

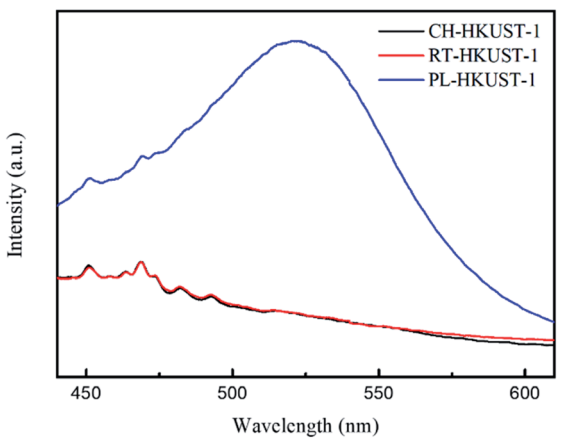

Fig. 2 FL spectra of CH-HKUST-1, RT-HKUST-1, and PL-HKUST-1 (λ_{ex} = 310 nm).

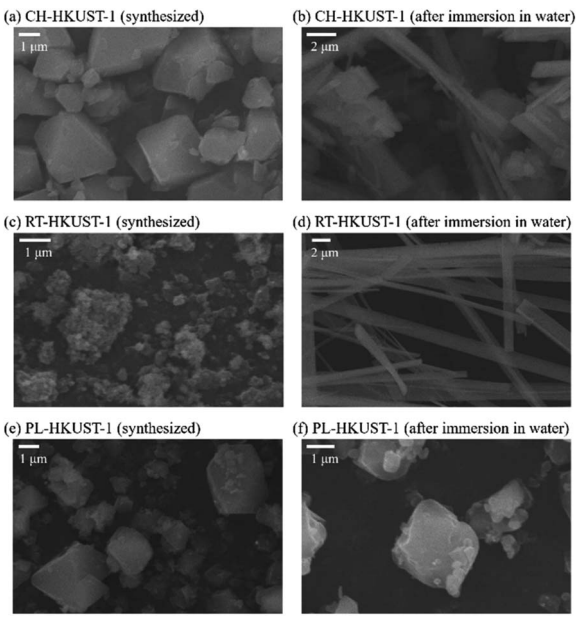

Fig. 3 SEM images of (a and b) CH-HKUST-1, (c and d) RT-HKUST-1, and (e and f) PL-HKUST-1 before and after immersion in water.

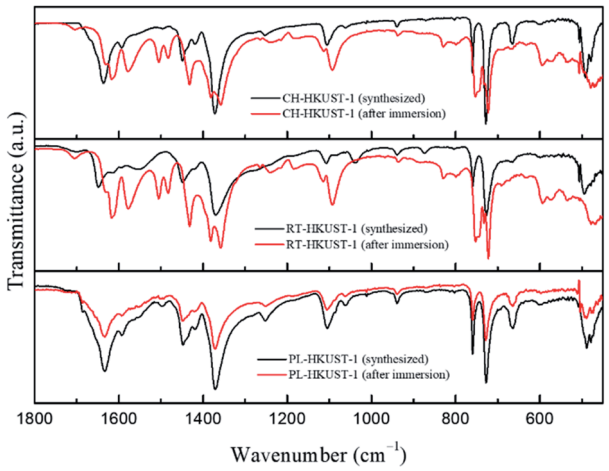

Fig. 4 FTIR spectra of CH-HKUST-1, RT-HKUST-1, and PL-HKUST-1 before and after immersion in water.

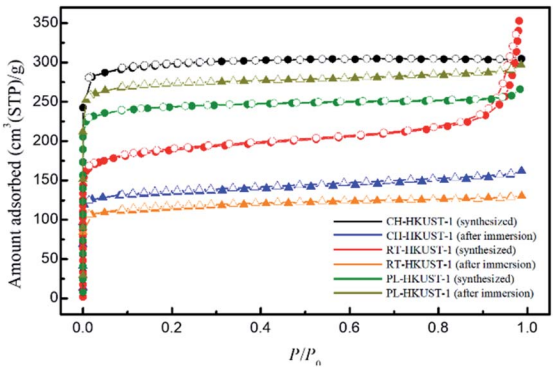

Fig. 5 N_2 adsorption (solid symbols) and desorption (open symbols) isotherms of CH-HKUST-1, RT-HKUST-1, and PL-HKUST-1 before and after immersion in water.

the range 1371–1448 cm^{-1} correspond to the symmetric stretching vibrations of the carboxylate group.[50] The bands at 730 and 758 cm^{-1} correspond to the in-plane C–H bending mode.[49] Peaks observed below 600 cm^{-1} correspond to the bonds involving copper ions.[49] After immersion in water, the FTIR spectrum of PL-HKUST-1 did not show any significant change whereas those of CH-HKUST-1 and RT-HKUST-1 showed shifts in the peaks and formation of new peaks. When exposed to water, peaks corresponding to COO vibrations were observed for CH-HKUST-1 and RT-HKUST-1 between 1200 and 1700 cm^{-1} due to a change in the environments of the linker BTC.[48] The peak around 1640 cm^{-1} shifted to longer wavelengths, and a new peak appeared around 1570 cm^{-1}, which is consistent with previous research.[38] The Raman spectra of CH-HKUST-1 and RT-HKUST-1 also showed the structural change in the coordination bonding upon the water treatment (Fig. S5†).[51]

Table 1 shows the Brunauer–Emmett–Teller (BET) surface areas for CH-HKUST-1, RT-HKUST-1, and PL-HKUST-1 obtained from the N_2 adsorption measurements (Fig. 5). The BET surface areas of CH-HKUST-1, RT-HKUST-1, and PL-HKUST-1 were 888, 574, and 739 m^2 g^{-1}, respectively. After immersion in water, the amount adsorbed by CH-HKUST-1 and RT-HKUST-1 was lowered compared to that before immersion, and their BET surface areas were 407 and 351 m^2 g^{-1}, respectively. By contrast, in the case of PL-HKUST-1, the adsorption amount remained high even after immersion in water, and its BET surface area was 811 m^2 g^{-1}.

These results clearly indicate that PL-HKUST-1 was more resistant to water than CH-HKUST-1 and RT-HKUST-1, and its high surface area could be retained for a longer period. This is because PL-HKUST-1 after immersion in water was not decomposed at all or at least under the midway in the decomposition process of HKUST-1. According to Todaro *et al.*, there are three stages in the decomposition of HKUST-1 during the adsorption of water molecules.[31] The first stage does not involve hydrolysis during the interaction with water molecules, triggering an irreversible modification. Under the present experimental conditions, the BET surface of PL-HKUST-1 did not decrease after immersion in water, indicating that it had not advanced beyond the reversible first stage. For CH-HKUST-1 and RT-HKUST-1, the large decrease in BET surface after exposure to water suggests that the reaction had progressed to the second or third stage of irreversible hydrolysis of the Cu–O bonds.

Table 1 Brunauer–Emmett–Teller surface areas of CH-HKUST-1, RT-HKUST-1, and PL-HKUST-1 before and after immersion in water

	Synthesized	After immersion
CH-HKUST-1	888 m^2 g^{-1}	407 m^2 g^{-1}
RT-HKUST-1	574 m^2 g^{-1}	351 m^2 g^{-1}
PL-HKUST-1	739 m^2 g^{-1}	811 m^2 g^{-1}

Various factors account for the higher water stability of PL-HKUST-1 compared to CH-HKUST-1 and RT-HKUST-1. One of the possible reasons is the higher concentration of Cu(I) in PL-HKUST-1. The mixture of Cu(II) and Cu(I) ions coordinated with BTC showed higher water stability,[36] although the structure changed due to the reduction. Our study indicates that PL-HKUST-1 still bears the HKUST-1 structure with Cu(I)-rich sites, similar to the MOF synthesized by reducing Cu(II) in HKUST-1 by heating, X-ray irradiation[45] or alcohol vapor treatment.[52] This may be due to the generation of missing-linker defects inside the structure of HKUST-1.[53] Due to the reduction, the state of open metal sites (OMS) might change, and their water adsorption might also be influenced.

It has also been reported that treatment of HKUST-1 with oxygen plasma prevents adsorption of water molecules. This is because the adsorption of oxygen on the OMS during plasma treatment prevents the adsorption of water in HKUST-1.[35] In this study, there were many radicals such as CH, OH, and O in the reaction field of plasma in liquid, which was confirmed from optical emission spectra (Fig. S6†); it is also possible that some species were adsorbed on the OMS, resulting in high water stability of PL-HKUST-1.

In conclusion, the results of this study revealed the applicability of plasma in liquid for MOF synthesis. Plasma was generated during the formation of HKUST-1, which allowed for uniform modification of the MOF crystals without using any

additives. Therefore, this method enabled us to obtain HKUST-1 with a higher Cu(I) content and high water stability compared to those synthesized by conventional synthetic methods. Since Cu(I) in HKUST-1 binds more strongly to adsorbed gases like nitrogen oxide than Cu(II),[54] it is expected to have potential applications for the development of gas separators with good gas selectivity. It has also been reported that mixed-valence copper sites increase the density of states near the Fermi level and thus increase the electrical conductivity.[45] In addition, MOFs with reduced Cu(I) ions are also expected to be used as catalysts for click reactions.[44] It may be possible to control the amount of reduced metal ions simply by tuning parameters such as irradiation time and plasma generation power. Further development of such systems, as well as their contribution to the preparation of novel functionalized MOFs, is expected in the future.

Conflicts of interest

There are no conflicts to declare.

Acknowledgements

We would like to thank Prof. Takashi Uemura (Univ. of Tokyo) for helpful discussions and comments on this manuscript. This work was partially supported by JSPS KAKENHI Grant No. 16H04506, 16H05988 and 19H01885.

Notes and references

1 C. Dey, T. Kundu, B. P. Biswal, A. Mallick and R. Banerjee, *Acta Crystallogr., Sect. B: Struct. Sci., Cryst. Eng. Mater.*, 2014, **70**, 3–10.
2 H. Furukawa, K. E. Cordova, M. O'Keeffe and O. M. Yaghi, *Science*, 2013, **341**, 1230444.
3 O. K. Farha, A. Özgür Yazaydın, I. Eryazici, C. D. Malliakas, B. G. Hauser, M. G. Kanatzidis, S. T. Nguyen, R. Q. Snurr and J. T. Hupp, *Nat. Chem.*, 2010, **2**, 944–948.
4 L. J. Murray, M. Dincă and J. R. Long, *Chem. Soc. Rev.*, 2009, **38**, 1294–1314.
5 J. Lee, O. K. Farha, J. Roberts, K. A. Scheidt, S. T. Nguyen and J. T. Hupp, *Chem. Soc. Rev.*, 2009, **38**, 1450–1459.
6 J. Ye and C. Liu, *Chem. Commun.*, 2011, **47**, 2167–2169.
7 W. Cai, C.-C. Chu, G. Liu and Y.-X. J. Wáng, *Small*, 2015, **11**, 4806–4822.
8 P. Horcajada, T. Chalati, C. Serre, B. Gillet, C. Sebrie, T. Baati, J. F. Eubank, D. Heurtaux, P. Clayette, C. Kreuz, J.-S. Chang, Y. K. Hwang, V. Marsaud, P.-N. Bories, L. Cynober, S. Gil, G. Férey, P. Couvreur and R. Gref, *Nat. Mater.*, 2010, **9**, 172–178.
9 Y. Cui, H. Xu, Y. Yue, Z. Guo, J. Yu, Z. Chen, J. Gao, Y. Yang, G. Qian and B. Chen, *J. Am. Chem. Soc.*, 2012, **134**, 3979–3982.
10 B. Chen, Y. Yang, F. Zapata, G. Lin, G. Qian and E. B. Lobkovsky, *Adv. Mater.*, 2007, **19**, 1693–1696.
11 S. Najafi Nobar, *Mater. Chem. Phys.*, 2018, **213**, 343–351.
12 K. Schlichte, T. Kratzke and S. Kaskel, *Microporous Mesoporous Mater.*, 2004, **73**, 81–88.
13 N. A. Khan, E. Haque and S. H. Jhung, *Phys. Chem. Chem. Phys.*, 2010, **12**, 2625–2631.
14 C. McKinstry, E. J. Cussen, A. J. Fletcher, S. V. Patwardhan and J. Sefcik, *Chem. Eng. J.*, 2017, **326**, 570–577.
15 N. A. Khan and S.-H. Jhung, *Bull. Korean Chem. Soc.*, 2009, **30**, 2921–2926.
16 M. R. Armstrong, S. Senthilnathan, C. J. Balzer, B. Shan, L. Chen and B. Mu, *Ultrason. Sonochem.*, 2017, **34**, 365–370.
17 M. Klimakow, P. Klobes, A. F. Thünemann, K. Rademann and F. Emmerling, *Chem. Mater.*, 2010, **22**, 5216–5221.
18 R. Senthil Kumar, S. Senthil Kumar and M. Anbu Kulandainathan, *Microporous Mesoporous Mater.*, 2013, **168**, 57–64.
19 S. Loera-Serna, M. A. Oliver-Tolentino, Ma. de Lourdes López-Núñez, A. Santana-Cruz, A. Guzmán-Vargas, R. Cabrera-Sierra, H. I. Beltrán and J. Flores, *J. Alloys Compd.*, 2012, **540**, 113–120.
20 X. Tao, C. Sun, Y. Han, L. Huang and D. Xu, *CrystEngComm*, 2019, **21**, 2541–2550.
21 X. Tao, W. Cong, L. Huang and D. Xu, *J. Alloys Compd.*, 2019, **805**, 1060–1070.
22 J. Kang, O. L. Li and N. Saito, *Carbon*, 2013, **60**, 292–298.
23 N. Matsuda, T. Nakashima, T. Kato and H. Shiroishi, *Electrochim. Acta*, 2014, **146**, 73–78.
24 T. Kaneko, K. Baba, T. Harada and R. Hatakeyama, *Plasma Processes Polym.*, 2009, **6**, 713–718.
25 N. Treesukkasem, C. Chokradjaroen, S. Theeramunkong, N. Saito and A. Watthanaphanit, *ACS Appl. Nano Mater.*, 2019, **2**, 8051–8062.
26 T. Goto, M. Iida, H. Tan, C. Liu, K. Mayumi, R. Maeda, K. Kitahara, K. Hatakeyama, T. Ito, Y. Shimizu, H. Yokoyama, K. Kimura, K. Ito, Y. Hakuta and K. Terashima, *Appl. Phys. Lett.*, 2018, **112**, 101901.
27 P. J. Bruggeman, M. J. Kushner, B. R. Locke, J. G. E. Gardeniers, W. G. Graham, D. B. Graves, R. C. H. M. Hofman-Caris, D. Maric, J. P. Reid, E. Ceriani, D. Fernandez Rivas, J. E. Foster, S. C. Garrick, Y. Gorbanev, S. Hamaguchi, F. Iza, H. Jablonowski, E. Klimova, J. Kolb, F. Krcma, P. Lukes, Z. Machala, I. Marinov, D. Mariotti, S. Mededovic Thagard, D. Minakata, E. C. Neyts, J. Pawlat, Z. L. Petrovic, R. Pflieger, S. Reuter, D. C. Schram, S. Schröter, M. Shiraiwa, B. Tarabová, P. A. Tsai, J. R. R. Verlet, T. von Woedtke, K. R. Wilson, K. Yasui and G. Zvereva, *Plasma Sources Sci. Technol.*, 2016, **25**, 053002.
28 P. Krawiec, M. Kramer, M. Sabo, R. Kunschke, H. Fröde and S. Kaskel, *Adv. Eng. Mater.*, 2006, **8**, 293–296.
29 H. Dathe, E. Peringer, V. Roberts, A. Jentys and J. A. Lercher, *C. R. Chim.*, 2005, **8**, 753–763.
30 J. Raziel Álvarez, E. Sánchez-González, E. Pérez, E. Schneider-Revueltas, A. Martínez, A. Tejeda-Cruz, A. Islas-Jácome, E. González-Zamora and I. A. Ibarra, *Dalton Trans.*, 2017, **46**, 9192–9200.
31 M. Todaro, G. Buscarino, L. Sciortino, A. Alessi, F. Messina, M. Taddei, M. Ranocchiari, M. Cannas and F. M. Gelardi, *J. Phys. Chem. C*, 2016, **120**, 12879–12889.
32 D.-D. Zu, L. Lu, X.-Q. Liu, D.-Y. Zhang and L.-B. Sun, *J. Phys. Chem. C*, 2014, **118**, 19910–19917.

33 B. Yuan, X.-Q. Yin, X.-Q. Liu, X.-Y. Li and L.-B. Sun, *ACS Appl. Mater. Interfaces*, 2016, **8**, 16457–16464.
34 J. B. Decoste, G. W. Peterson, M. W. Smith, C. A. Stone and C. R. Willis, *J. Am. Chem. Soc.*, 2012, **134**, 1486–1489.
35 J. Bae, J.-W. Jung, H. Yul Park, C.-H. Cho and J. Park, *Chem. Commun.*, 2017, **53**, 12100–12103.
36 A. Ahmed, C. M. Robertson, A. Steiner, T. Whittles, A. Ho, V. Dhanak and H. Zhang, *RSC Adv.*, 2016, **6**, 8902–8905.
37 Z.-Q. Li, L.-G. Qiu, T. Xu, Y. Wu, W. Wang, Z.-Y. Wu and X. Jiang, *Mater. Lett.*, 2009, **63**, 78–80.
38 J. B. DeCoste, G. W. Peterson, B. J. Schindler, K. L. Killops, M. A. Browe and J. J. Mahle, *J. Mater. Chem. A*, 2013, **1**, 11922–11932.
39 S. Evariste, A. M. Khalil, M. E. Moussa, A. K.-W. Chan, E. Y.-H. Hong, H.-L. Wong, B. Le Guennic, G. Calvez, K. Costuas, V. W.-W. Yam and C. Lescop, *J. Am. Chem. Soc.*, 2018, **140**, 12521–12526.
40 A. Liske, L. Wallbaum, T. Hölzel, J. Föller, M. Gernert, B. Hupp, C. Ganter, C. M. Marian and A. Steffen, *Inorg. Chem.*, 2019, **58**, 5433–5445.
41 S. Shi, M. C. Jung, C. Coburn, A. Tadle, M. R. Daniel Sylvinson, P. I. Djurovich, S. R. Forrest and M. E. Thompson, *J. Am. Chem. Soc.*, 2019, **141**, 3576–3588.
42 L. Lv, K. Yuan, Y. Zhu, G. Zuo and Y. Wang, *J. Phys. Chem. A*, 2019, **123**, 2080–2090.
43 H. Sun, X. Han, K. Liu, B. Shen, J. Liu, D. Wu and X. Shi, *Ind. Eng. Chem. Res.*, 2017, **56**, 9541–9550.
44 Q. Fu, K. Xie, S. Tan, J. M. Ren, Q. Zhao, P. A. Webley and G. G. Qiao, *Chem. Commun.*, 2016, **52**, 12226–12229.
45 A. S. Duke, E. A. Dolgopolova, R. P. Galhenage, S. C. Ammal, A. Heyden, M. D. Smith, D. A. Chen and N. B. Shustova, *J. Phys. Chem. C*, 2015, **119**, 27457–27466.
46 F. Rezaei, P. Vanraes, A. Nikiforov, R. Morent and N. De Geyter, *Materials*, 2019, **12**, 2751.
47 J. Szanyi, M. Daturi, G. Clet, D. R. Baer and C. H. F. Peden, *Phys. Chem. Chem. Phys.*, 2012, **14**, 4383–4390.
48 G. Majano, O. Martin, M. Hammes, S. Smeets, C. Baerlocher and J. Pérez-Ramírez, *Adv. Funct. Mater.*, 2014, **24**, 3855–3865.
49 Z. Dong, Z. Mi, W. Shi, H. Jiang, Y. Zheng and K. Yang, *RSC Adv.*, 2017, **7**, 55504–55512.
50 R. Lin, L. Ge, H. Diao, V. Rudolph and Z. Zhu, *ACS Appl. Mater. Interfaces*, 2016, **8**, 32041–32049.
51 C. Prestipino, L. Regli, J. G. Vitillo, F. Bonino, A. Damin, C. Lamberti, A. Zecchina, P. L. Solari, K. O. Kongshaug and S. Bordiga, *Chem. Mater.*, 2006, **18**, 1337–1346.
52 S.-C. Qi, X.-Y. Qian, Q.-X. He, K.-J. Miao, Y. Jiang, P. Tan, X.-Q. Liu and L.-B. Sun, *Angew. Chem., Int. Ed.*, 2019, **58**, 10104–10109.
53 K. Müller, K. Fink, L. Schöttner, M. Koenig, L. Heinke and C. Wöll, *ACS Appl. Mater. Interfaces*, 2017, **9**, 37463–37467.
54 N. Nijem, H. Bluhm, M. L. Ng, M. Kunz, S. R. Leone and M. K. Gilles, *Chem. Commun.*, 2014, **50**, 10144–10147.